Stability of 100 Homo and Heterotypic Coiled−Coil **a**−**a′** Pairs for Ten Amino Acids (A, L, I, V, N, K, S, T, E, and R)

Asha Acharya, Vikas Rishi, and Charles Vinson*

Laboratory of Metabolism, National Cancer Institute, National Institutes of Health, Bethesda, Maryland 20892

Received April 26, 2006; Revised Manuscript Received August 2, 2006

ABSTRACT: We present the thermal stability monitored by circular dichroism (CD) spectroscopy at 222 nm of 100 heterodimers that contain all possible coiled-coil **a**−**a′** pairs for 10 amino acids (I, V, L, N, A, K S, T, E, and R). This includes the stability of 36 heterodimers for 6 amino acids (I, V, L, N, A, and K) previously described (*1*) and 64 new heterodimers including the 4 amino acids (S, T, E, and R). We have calculated a double mutant alanine thermodynamic cycle to determine **a**−**a′** pair coupling energies to evaluate which **a**−**a′** pairs encourage specific dimerization partners. The four new homotypic **a**−**a′** pairs (T−T, S−S, R−R, E−E) are repulsive relative to A−A and have destabilizing coupling energies. Among the 90 heterotypic **a**−**a′** pairs, the stabilizing coupling energies contain lysine or arginine paired with either an aliphatic or a polar amino acid. The range in coupling energies for each amino acid reveals its potential to regulate dimerization specificity. The **a**−**a′** pairs containing isoleucine and asparagine have the greatest range in coupling energies and thus contribute dramatically to dimerization specificity, which is to encourage homodimerization. In contrast, the **a**−**a′** pairs containing charged amino acids (K, R, and E) show the least range in coupling energies and promiscuously encourage heterodimerization.

The coiled-coil structure (*2*, *3*), a repeating amphipathic α-helix that multimerizes is found in about 3% of all proteins (*4*, *5*). The dimeric parallel coiled-coil structure repeats every two α-helical turns or seven amino acids with each amino acid position identified using the nomenclature (**a**,**b**,**c**,**d**,**e**,**f**,**g**)$_n$ (*6*). Coiled-coil dimers are mainly stabilized by the hydrophobic core created by the typically hydrophobic **a** and **d** residues (*7*) that pack in a regular knobs and holes pattern along the dimerization interface (*3*).

The basic leucine zipper (B-ZIP[1]) class of sequence-specific transcription factors, which has 53 human members (*8*), uses a parallel coiled-coil as a dimerization domain termed the leucine zipper because of a leucine repeat every seven amino acids (*9*). B-ZIP proteins can either homodimerize and/or heterodimerize (*10*). These dimerization domains are typically four to five heptads long and contain amino acids that maximize their stability. The leucine zipper sequences found in B-ZIP proteins may represent trigger sequences that initiate protein folding in longer coiled coils (*11*, *12*).

To evaluate amino acids involved in regulating the dimerization specificity of parallel dimeric coiled coils, we and others have determined the contribution of amino acids at the dimerization interface to stability and specificity (*13*−*15*). We have been systematically determining the contribution of individual amino acids in the **g**, **a**, **d**, and **e** positions of the 3rd and 4th heptads of the VBP leucine zipper for both dimerization stability and specificity (*1*, *16*−*19*). The **d** position is typically leucine, contributing to dimerization stability but not to specificity (*17*). In contrast, the **a** position is more variable and, thus, may contribute to both dimerization stability and specificity. However, changing amino acids in the **a** position can modulate oligomerization, particularity of the GCN4 leucine zipper (*14*, *20*−*22*), complicating the analysis of the contribution of amino acids in the **a** position to dimerization specificity.

Previously, we examined the contribution of six amino acids (A, V, I, L, N, and K) in homotypic **a**−**a′** pairs and heterotypic (different amino acids in the **a** and **a′** positions) **a**−**a′** pairs using a heterodimerizing leucine zipper system (*1*). We have extended this analysis to include four additional amino acids (S, T, E, and R) that are often found in the **a** position of leucine zippers. We now present the thermal stability of 64 more heterodimers for a total of 100 heterodimers that contain all combinations of these 10 amino acids in **a**−**a′** pairs. Using an alanine based double mutant thermodynamic cycle calculation, we have determined the coupling energy between amino acids in the **a**−**a′** pair to gain insight into amino acid interactions that regulate coiled-coil dimerization specificity. These data should be valuable for coiled-coil design (*23*), predicting coiled-coil dimerization specificity (*24*), and calibrating computation models of coiled-coil stability (*25*).

EXPERIMENTAL PROCEDURES

Proteins. The heterodimerizing protein system used in this study is described previously (*1*). Heterodimerizing proteins B-EE$_{34}$ (X) and A-RR$_{34}$ (X) are derived from the chicken VBP protein (*26*). The amino acid sequence of the 96 amino acid B-EE$_{34}$ (X) protein is ASMTGGQQMGRDP-LEE KVFVPDEQKDEKYW TRRKKNNVAAK RSRDARRL

* Corresponding author: Tel: (301) 496-8753. Fax: (301) 496-8419. E-mail: Vinsonc@mail.nih.gov.

[1] Abbreviations: B-ZIP, basic leucine zipper; CD, circular dichroism; T_m, midpoint of thermal denaturation; ΔH_m, enthalpy change at T_m; ΔG_{37}, Gibbs free energy change at 37 °C.

10.1021/bi060822u CCC: $33.50
Published on Web 09/02/2006

KENQITI RAAFLEK ENTALRT **EX**AEL**E**K **E**VGRC**E**N IVSKYE TRYGPL. The leucine zipper region has been grouped into heptads (**gabcdef**). In B-EE_{34} (X), B- represents the basic region, EE_{34} represents the VBP leucine zipper with the 3rd and 4th **g↔e′** pairs containing repulsive E↔E pairs, and (X) represents the guest−host position amino acid in the 3rd **a** position. In the protein sequence of B-EE_{34} (X), the four glutamic acids in bold produce two repulsive E↔E pairs in the 3rd and 4th heptads that preclude the formation of a stable homodimer. The amino acid sequence of A-RR_{34} (X) is ASMTGGQQMGRDP-LEE-LEQRAEELAREN EE-LEKEAEELEQENAELEI RAAFLEK ENTALRT **RX**AEL-**R**K **R**VGRC**R**N IVSKYETRYGPL. In A-RR_{34}(X), A- represents the acidic extension that can form a coiled-coil heterodimeric structure with the VBP basic region (*26*), RR_{34} represents the leucine zipper with the 3rd and 4th **g↔e′** pairs containing repulsive R↔R pairs, and (X) represents the guest−host position amino acid in the 3rd **a** position. The four arginines (in bold) in the 3rd and 4th heptads produce repulsive R↔R pairs and prevent homodimerization.

Protein Purification. Proteins were expressed in *E. coli* BL21 lysE cells using the T7 IPTG-inducible system (*27*). The B-EE_{34} (X) and A-RR_{34} (X) proteins were purified as described previously (*28*).

Circular Dichroism. Circular dichroism (CD) studies were performed using a Jasco J-720 spectropolarimeter with a 5-mm rectangular CD cell. All protein samples were in 12.5 mM potassium phosphate (pH 7.4), 150 mM KCl, and 0.25 mM EDTA. For the assay, 1 mM DTT was added to the protein solution and heated to 65 °C for 15 min to disrupt the potential disulfide bond that can form between the two cysteine residues in the **d** position in the 4th heptad, cooled to room temperature for 5 min, and diluted to 2 μM in 1.5 mL of stock buffer (described above). Wavelength scans were performed at 6 °C from 260 to 200 nm. Temperature denaturation studies continuously monitored molar ellipticity at 222 nm from 6 °C to 80 °C at a scan rate of 1 °C/min.

Thermodynamic Calculations. Melting temperature (T_m) and enthalpy change at melting temperature (ΔH_m) values were determined from denaturation curves assuming a two-state equilibrium dissociation of α-helical dimers into unfolded monomers using the following equation (for details see ref 16 (*16*)).

$$-[\theta]_{222}(T) = (N - D)\,(1 - T/T_{inter})\,[1 + 1 - (8\exp\{\Delta H_m\,(1/T_m - 1/T)/R + 1\})^{1/2}/4\exp\Delta H_m(1/T_m - 1/T)/R] + D \quad (1)$$

where $\theta_{222}(T)$ is ellipticity at 222 nm at any temperature (°C), N is the ellipticity of the dimer at 0 °C, D is the ellipticity at high temperature at which all of the protein molecules are assumed to be unhelical monomers, T_{intr} is the temperature at which the linear temperature-dependencies of dimer and monomer molecules intersect, and R is the gas constant. Each thermal denaturation curve was fitted to five parameters (N, D, T_{intr}, T_m, and ΔH_m).

The standard errors for T_m and ΔH_m determined from the fitting procedure were typically not higher than 0.3 °C and 1.5 kcal/mol/dimer, respectively. Constant-pressure heat capacity change (ΔC_p) was calculated using the T_m versus ΔH_m plot for the 100 heterodimer denaturations, 64 denaturations presented in this manuscript and the 36 denaturations reported earlier (*1*). A linear fitting of these data has a slope (ΔC_p) of -2.18 ± 0.19 kcal/mol/dimer/°C that was used in Gibbs−Helmholtz equation to calculate ΔG_{37} (Gibbs free energy change at 37 °C) values for each of the 100 denaturations. Previously, the ΔC_p calculated for the 36 denaturations was -2.04 ± 0.19 kcal/mol/dimer/°C, but this difference in ΔC_p, however, did not affect the calculated ΔG_{37} values to two decimal points.

Transfer free energies for amino acids at 25 °C (*29*) were extrapolated to 37 °C, resulting in energies relative to those of alanine in kcal/mol for I = −2.1; V = −1.3; L = −2.0; N = 1.3; T = 0.1; S = 0.5; K = 1.8; R = 1.9; and E = 1.4.

RESULTS

Design of Heterodimerizing Leucine Zippers. Figure 1 presents a side and end view cartoon of the heterodimerizing guest−host system containing the B-EE_{34}(X) and A-RR_{34}-(X) monomers that we used to produce both homotypic and heterotypic **a**−**a′** pairs (*1*). In this system, B-EE_{34}(X) contains glutamic acids in the 3rd and 4th heptads in both the **g** and **e** positions. In contrast, A-RR_{34}(X) contains arginine in the 3rd and 4th heptads in both the **g** and **e** positions. These amino acids contribute to the heterodimerization of B-EE_{34}-(X)|A-RR_{34}(X) by producing attractive **g↔e′** pairs (*16*). To add additional heterodimerization determinants to this heterodimerizing system, the basic region of B-RR_{34}(X) was replaced with an acidic and amphipathic protein sequence to generate A-RR_{34}(X) (*8*, *23*, *26*). This acidic extension forms a coiled-coil structure with the basic region of B-EE_{34}-(X). All of these structural elements favor heterodimerization of this guest host system as confirmed previously by analytical ultracentrifugation (*1*).

The guest−host position is the 3rd heptad **a** position and is flanked by leucines in the 2nd and 3rd heptad **d** positions, producing a canonical hydrophobic interface. The overlaying two attractive interhelical **g↔e′** pairs are not identical; in the B-EE_{34}(X)|A-RR_{34}(X) heterodimer, one surface contains two **E↔R g↔e′** pairs, whereas the opposite surface contains two **R↔E g↔e′** pairs. Consequently, when we make reciprocal **a**−**a′** pairs, for example, by the B-EE_{34}(T)|A-RR_{34}-(S) heterodimer or the B-EE_{34}(S)|A-RR_{34}(T) heterodimer to produce a T−S and S−T **a**−**a′** pair, respectively, these reciprocal heterotypic **a**−**a′** pairs are not structurally equivalent as would occur if the overlaying **g↔e′** pairs were formed in a homodimer. Thus, we can evaluate whether the orientation of the overlaying **g↔e′** pairs affect the stability of reciprocal heterotypic **a**−**a′** pairs.

Figure 2A shows three circular dichroism (CD) spectra from 260 to 200 nm for the B-EE_{34}(T) homodimer, the A-RR_{34}(T) homodimer, and the B-EE_{34}(T)|A-RR_{34}(T) heterodimer. All 100 heterodimers have spectra with minima at 208 nm and 222 nm that are characteristic of α-helices and α-helical interactions, respectively (*30*). The ratio of ellipticities (222/208 nm) is greater than 1.0 for all B-EE_{34} (X)|A-RR_{34}(X) heterodimers, indicative of interactions between α-helices such as occurs in a coiled-coil structure (*31*, *32*). The ellipticity of the mixture is greater than the sum of the individual samples, suggesting the formation of an α-helical coiled-coil structure between the basic region of B-EE_{34} (T) and the acidic region of A-RR_{34} (T).

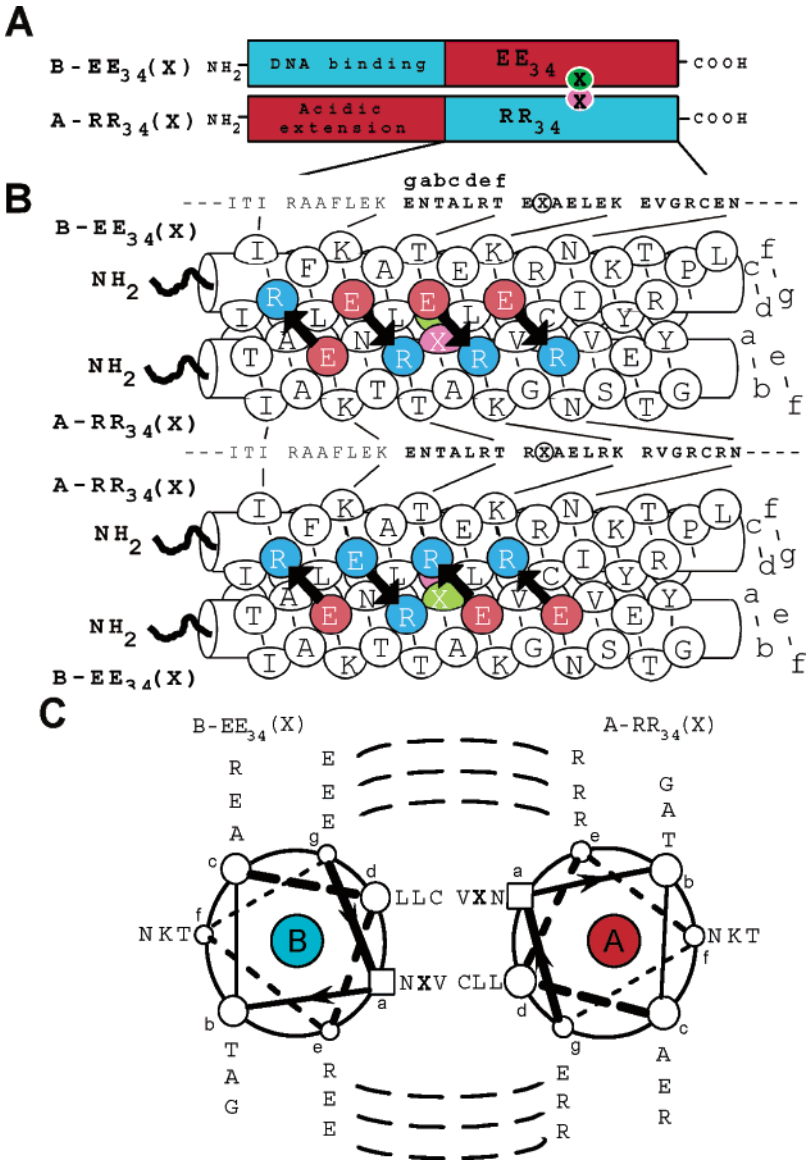

FIGURE 1: (A) Schematic diagram of the guest−host B-EE$_{34}$(X)|A-RR$_{34}$(X) heterodimer. B-EE$_{34}$(X) has the basic DNA binding region and leucine zipper containing repulsive **E↔E g↔e′** pairs. A-RR$_{34}$(X) has an acidic extension and leucine zipper containing repulsive **R↔R g↔e′** pairs. The guest−host position is in the 3rd heptad **a** position and is shown as a circle with an X inside. (B) Side view of the heterodimerizing leucine zipper with each amino acid position shown as a circle. An arrow connects amino acids in the **g** and **e** position as they form attractive **g↔e′** pairs. The letters to the right of the coiled-coil schematic are the coiled-coil positions (a,b,c,d,e,f,g). The two strings of letters on the top and bottom of the first schematic are the amino acid sequences of the leucine zipper region of B-EE$_{34}$(X) and A-RR$_{34}$(X) grouped into heptads (**g**,a,b,c,d,e,f). The three heptads in bold are shown again in panel C. These strings do not include the final 12 amino acids (IVSKYEY RYGPL) of the heterodimerizing leucine zippers. (C) End view of the coiled-coil structure viewed from the *N*-terminus showing the 3 heptads of amino acids and the standard coiled-coil nomenclature for the seven unique positions of the coiled-coil heptad. Potential attractive interhelical **g↔e′** pairs are shown with dashed lines and the guest−host position is shown as an X.

Figure 2B shows thermal denaturations monitored by circular dichroism spectroscopy at 222 nm of the three samples presented in Figure 2A. The B-EE$_{34}$(T) homodimer and the A-RR$_{34}$(T) homodimer have T_m values of ∼6.1 °C and ∼8.0 °C, respectively, whereas the B-EE$_{34}$(T)|A-RR$_{34}$-(T) heterodimer is over 33 °C more stable with a T_m of 41 °C, demonstrating the preferential heterodimer formation in the mixture. The preferential formation of heterodimers when the two proteins are mixed allows for the energetic determination of unfavorable heterotypic **a**−**a′** interactions.

Stability of 100 B-EE$_{34}$(X)|A-RR$_{34}$(X) Heterodimers. We have extended our previous analysis of the energetic contribution of six amino acids (A, I, L, V, N, and K) to homotypic and heterotypic **a**−**a′** interactions (*1*) to include four more amino acids (S, T, R, and E) that are commonly observed in the **a** position of both human (∼10%) (*8*) and *Arabadopsis* (∼15%) (*19*) B-ZIP leucine zippers (Figure 3). In total, these 10 amino acids represent 90% and 80% of amino acids observed in the **a** position of human and *Arabadopsis* B-ZIP leucine zippers, respectively. Table 1 shows thermodynamic parameters calculated from thermal denaturations monitored by circular dichroism spectroscopy at 222 nm for 64 new heterodimers that contain both homotypic and heterotypic **a**−**a′** interactions. The spectra from 260 to 200 nm and thermal denaturation profiles for all 100 heterodimers are given as Supporting Information. These denaturations are well fit by a two-state denaturation

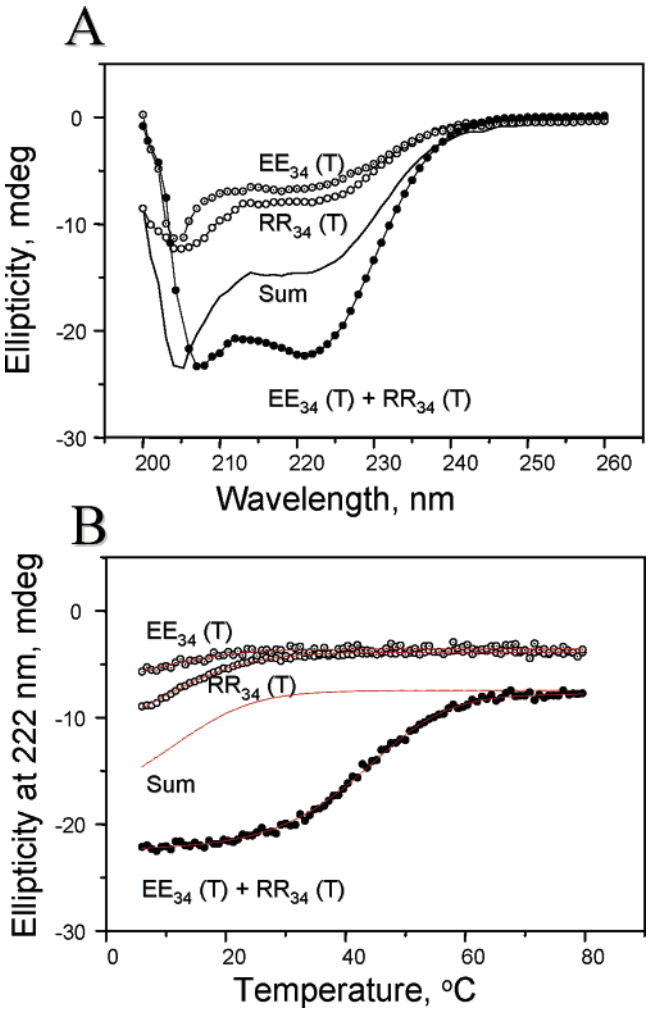

FIGURE 2: (A) Circular dichroism spectra from 200 to 260 nm of 2 μM B-EE$_{34}$ (T), 2 μM A-RR$_{34}$(T), and the equimolar mixture of 2 μM B-EE$_{34}$(T) and 2 μM A-RR$_{34}$(T). The sum curve is the assumed spectrum if the two proteins do not interact. (B) Thermal denaturations monitored by circular dichroism spectroscopy at 222 nm of the three samples from panel A. The line through the data is a fitted curve assuming a two-state equilibrium. The sum curve is the assumed thermal denaturation if the two proteins do not interact. The B-EE$_{34}$(T) and A-RR$_{34}$(T) mixture is more stable than either protein alone, indicating that proteins are forming a B-EE$_{34}$-(T)|A-RR$_{34}$(T) heterodimer.

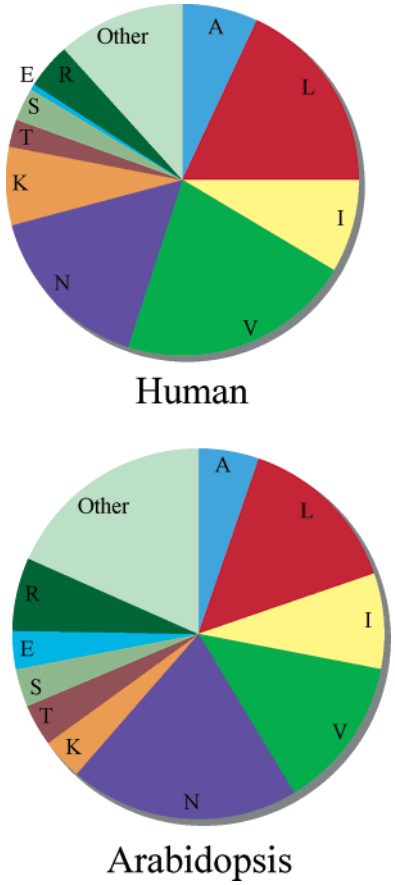

FIGURE 3: Frequency of amino acids in the **a** position of the leucine zipper of either human or *Arabadopsis* B-ZIP proteins (*19*). Eleven sectors are included, the 10 amino acids that have been examined experimentally plus the frequency of the remaining 10 amino acids summed in the 11nth sector.

model according to eq 1 giving values of T_m and ΔH_m. ΔG_{37} values were obtained using a ΔC_p value of −2.18±0.19 kcal/mol/dimer/°C calculated from all 100 heterodimers (Table 1). Figure 4 presents the thermal denaturations for the four heterodimer mixtures that produce homotypic **a**−**a′** pairs (S−S, T−T, R−R, and E−E). Only one of the 100 heterodimers producing the **a**−**a′** pair, E−E, was so unstable that it made the thermodynamic calculation questionable. The heterodimer B-EE$_{34}$ (E)|A-RR$_{34}$ (E) at 2 μM for each protein has a T_m of approximately 14 °C. To further evaluate the energetics of this thermal denaturation, we increased the protein concentration to 8.4 μM. This increased the T_m of the bimolecular reaction to 23 °C, whereas the calculated free energies were similar, −3.1 kcal/mol/dimer and −3.3 kcal/mol/dimer, respectively (Figure 5).

Table 2 presents the difference in stability between A−A, the **a**−**a′** pair with alanine in both **a** positions, and each of the remaining 99 **a**−**a′** pairs. The relative stabilities range from −9.2 kcal/mol/dimer for I−I to +6.0 kcal/mol/dimer for E−E. Using alanine as one of the two amino acids in the **a**−**a′** pair allowed us to examine the contribution of a single amino acid to stability without the confounding contribution of the second amino acid. In **a**−**a′** pairs containing alanine in A-RR$_{34}$ (A), 5 amino acids (I, V, L, N, and T) are more stabilizing than A−A, whereas 4 are less stabilizing (S, K, R, and E). Also, 41 heterotypic **a**−**a′** pairs are more stable than A−A, and 49 are less stable. All 25 heterotypic **a**−**a′** interactions between the 5 amino acids, S, T, K, R, and E, are less stable than A−A.

The 90 heterotypic **a**−**a′** pairs represent 45 reciprocal **a**−**a′** pairs that have overlying **g**↔**e′** pairs with the opposite orientation. Table 3 shows the difference in the stability for the 45 reciprocal heterotypic **a**−**a′** pairs. Some clear trends are observed. Heterotypic **a**−**a′** pairs containing the aliphatic amino acids (A, L, V, and I) do not show much difference in energy between reciprocal pairs (0.3 kcal/mol), suggesting they are not interacting with the overlying attractive **g**↔**e′** pairs. All heterotypic **a**−**a′** pairs containing one hydrophobic amino acid (A, I, V, and L) and one polar or basic amino acid (T, S, R, and K) are more stable when the polar or basic amino acid is in the acidic B-EE$_{34}$(X) background. In contrast, heterotypic **a**−**a′** pairs containing E are more stable with E in the A-RR$_{34}$ background. The greatest difference is observed for **a**−**a′** pairs containing threonine, where the difference can be as great as 1.5 kcal/mol/dimer for the T−N

Table 1: Thermal Stability of B-EE$_{34}$(X)|A-RR$_{34}$(X) Heterodimers with Different **a**−**a′** Pairs[a]

Thermal Stability of B-EE$_{34}$(X)|A-RR$_{34}$(X) Heterodimers

	A-RR$_{34}$(S)			A-RR$_{34}$(T)			A-RR$_{34}$(R)			A-RR$_{34}$(E)		
protein	T_m °C	ΔH_m kcal mol dimer	ΔG_{37} kcal mol dimer	T_m °C	ΔH_m kcal mol dimer	ΔG_{37} kcal mol dimer	T_m °C	ΔH_m kcal mol dimer	ΔG_{37} kcal mol dimer	T_m °C	ΔH_m kcal mol dimer	ΔG_{37} kcal mol dimer
B-EE$_{34}$(A)	36.8	−52.7	−7.9	34.5	−55.5	−8.4	25.9	−42.8	−7.3	26	−43.9	−7.5
B-EE$_{34}$(I)	47.9	−61.4	−10.1	46.8	−77.6	−10.1	49.4	−92.8	−11.2	48.1	−76.5	−10.5
B-EE$_{34}$(V)	47	−47.9	−8.7	48.2	−69.4	−10.0	45.1	−91.2	−9.8	41.8	−71.6	−9.1
B-EE$_{34}$(L)	46.1	−53.2	−8.9	44	−75.6	−9.7	43.2	−86.1	−9.5	43.6	−79.5	−9.4
B-EE$_{34}$(N)	39.1	−49.6	−7.9	42.2	−26.9	−8.0	39.1	−71.9	−8.3	34.3	−67.1	−7.4
B-EE$_{34}$(T)	38.3	−44.1	−7.6	40.8	−42.0	−8.5	36.6	−65.5	−7.8	35.6	−80.4	−7.3
B-EE$_{34}$(S)	37.5	−27.8	−7.5	27.4	−41.0	−6.7	25.7	−53.9	−7.0	22.7	−77.1	−7.1
B-EE$_{34}$(K)	36.4	−60.3	−7.3	35.9	−51.6	−7.3	21.1	−55.1	−5.4	20.8	−38.2	−6.0
B-EE$_{34}$(R)	24.2	−43.5	−6.6	24.7	−45.8	−6.9	20.1	−50.4	−5.1	20.2	−37.3	−5.5
B-EE$_{34}$(E)	20.2	−39.5	−5.2	21.7	−39.9	−6.0	19.7	−38.6	−5.0	13.5	−52.2	−3.1

Thermal Stability of B-EE$_{34}$(X)A-RR$_{34}$(X) Heterodimers

	B-EE34(S)			B-EE34(T)			B-EE34(R)			B-EE34(E)		
protein	T_m °C	ΔH_m kcal mol dimer	ΔG_{37} kcal mol dimer	T_m °C	ΔH_m kcal mol dimer	ΔG_{37} kcal mol dimer	T_m °C	ΔH_m kcal mol dimer	ΔG_{37} kcal mol dimer	T_m °C	ΔH_m kcal mol dimer	ΔG_{37} kcal mol dimer
A-RR34(A)	37.6	−54.7	−9.1	44.5	−81.9	−9.6	37.8	−67.4	−7.9	23.8	−41.1	−7.2
A-RR34(I)	47.6	−77.7	−10.5	49.7	−93.3	−11.4	50.9	−91.5	−12.1	46.5	−74.3	−9.8
A-RR34(V)	47.1	−49.6	−8.9	49.6	−90.2	−11.2	44.8	−75.3	−10.6	41.4	−69.5	−8.5
A-RR34(L)	47.2	−51.0	−9.1	49.1	−83.1	−10.6	47.3	−81.2	−10.3	42.3	−78.2	−8.7
A-RR34(N)	43.9	−82.2	−9.5	43.1	−88.6	−9.5	40.2	−51.3	−9.1	23.1	−40.2	−7.0
A-RR34(T)	27.4	−41.0	−6.7	40.8	−42.0	−8.5	24.7	−45.8	−6.9	21.7	−39.9	−6.0
A-RR34(S)	37.2	−27.8	−7.5	38.3	−44.1	−7.6	24.2	−43.5	−6.6	20.2	−39.5	−5.2
A-RR34(K)	35.5	−69.0	−7.6	40.9	−77.2	−8.6	20.3	−52.5	−5.2	20	−41.9	−5.5
A-RR34(R)	25.7	−53.9	−7.0	36.6	−65.5	−7.8	20.1	−50.4	−5.1	19.7	−38.6	−5.0
A-RR34(E)	22.7	−77.1	−7.1	35.6	−80.4	−7.3	20.2	−37.3	−5.5	13.5	−52.2	−3.1

[a] The table presents thermodynamic characterizations of the thermal denaturation profiles assuming a two-state denaturation: the thermal stability measured by circular dichroism at 222 nm, including melting temperature (T_m, °C), enthalpy change at melting temperature (ΔH_m, kcal/mol/dimer), and dimerization free energy extrapolated to 37 °C (ΔG_{37} in kcal/mol/dimer). The error in T_m and ΔH_m values is due to the error in fitting according to eq 1 and is <0.3 °C and 1.5 kcal/mol/dimer, respectively for all measurements.

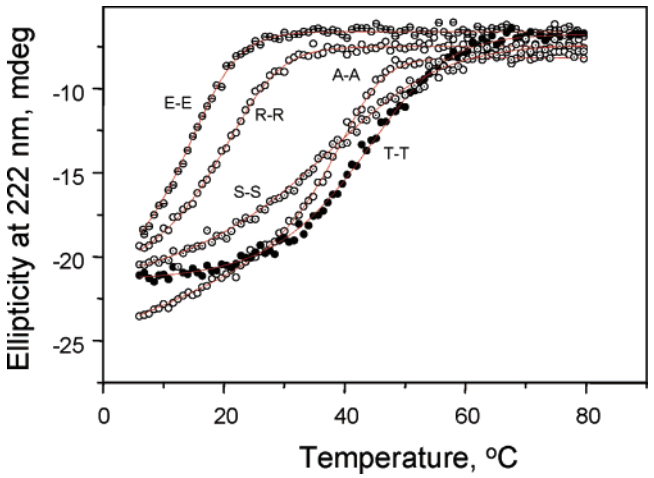

FIGURE 4: Thermal denaturations curves of five heterodimer mixtures formed by mixing B-EE$_{34}$(X) and A-RR$_{34}$(X) producing four homotypic **a**−**a′** interactions (E−E, R−R, A−A, S−S, and T−T).

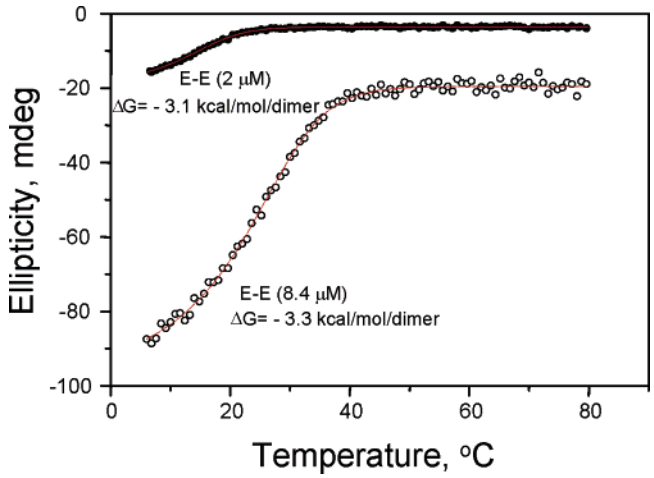

FIGURE 5: Thermal denaturations of the protein mixture B-EE$_{34}$-(E) and A-RR$_{34}$(E) at 2 and 8.4 μM monitored by circular dichroism spectroscopy at 222 nm.

a−**a′** pair. These results suggest that some amino acids in the **a** position energetically interact differentially with the overlying **E**↔**R** or **R**↔**E** pairs.

Coupling Energies for a−*a′ Pairs.* Table 4 shows the coupling energies for **a**−**a′** pairs derived from an alanine based double mutant thermodynamic cycle analysis (*33*). Twenty-four **a**−**a′** pairs have attractive coupling energies, and 57 have repulsive coupling energies. The four new homotypic **a**−**a′** coupling energies are repulsive (positive) with T−T and S−S being close to zero (+0.2 kcal/mol/dimer), whereas the coupling energies for R−R and E−E are more repulsive at +1.2 and +2.1 kcal/mol/dimer, respectively. All attractive coupling energies are smaller than 1.0 kcal/mol/dimer, whereas the repulsive coupling energy is as great as 4.9 kcal/mol/dimer for the I−N pair. The 24

Table 2: Energetic Difference for **a**−**a′** Pairs Relative to A−A[a]

	a−**a′** Pair stability (kcal/mol/dimer) relative to A−A									
protein	A-RR34(A) $\Delta\Delta G_{37}$	A-RR34(I) $\Delta\Delta G_{37}$	A-RR34(V) $\Delta\Delta G_{37}$	A-RR34(L) $\Delta\Delta G_{37}$	A-RR34(N) $\Delta\Delta G_{37}$	A-RR34(T) $\Delta\Delta G_{37}$	A-RR34(S) $\Delta\Delta G_{37}$	A-RR34(K) $\Delta\Delta G_{37}$	A-RR34(R) $\Delta\Delta G_{37}$	A-RR34(E) $\Delta\Delta G_{37}$
B-EE34(A)	0	−4.0	−2.4	−2.3	−1.0	+0.9	+1.4	+1.6	+2.0	+1.8
B-EE34(I)	−4.3	−9.2	−6.3	−5.7	−0.4	−0.8	−0.8	−3.1	−1.9	−1.2
B-EE34(V)	−2.3	−6.1	−5.4	−4.4	−0.1	−0.7	+0.6	−1.2	−0.5	+0.2
B-EE34(L)	−2.3	−5.8	−4.5	−5.2	−0.5	−0.4	+0.4	−0.8	−0.2	−0.1
B-EE34(N)	−0.9	−0.6	−0.3	−0.6	−2.4	+1.3	+1.4	+0.5	+1.0	+1.9
B-EE34(T)	−0.3	−2.1	−1.9	−1.3	−0.2	+0.8	+1.7	+0.7	+1.5	+2.0
B-EE34(S)	+0.2	−1.2	+0.4	+0.2	−0.2	+2.6	+1.8	+1.7	+2.3	+2.2
B-EE34(K)	+1.0	−3.7	−1.9	−1.5	−0.3	+2.0	+2.0	+2.9	+3.9	+3.3
B-EE34(R)	+1.4	−2.8	−1.3	−1.0	+0.2	+2.4	+2.7	+4.1	+4.6	+3.8
B-EE34(E)	+2.1	−0.5	+0.8	+0.6	+2.3	+3.3	+4.1	+3.8	+4.3	+6.0

[a] The difference in the thermal stabilities of 99 heterodimers relative to that of B-EE_{34}(A)|A-RR_{34}(A) are calculated from the ΔG_{37} values in Table 1 or our previous publication (*1*). For example, ΔG_{37} difference ($\Delta\Delta G_{37}$) between B-EE_{34}(S)|A-RR_{34}(S) and B-EE_{34}(A)|A-RR_{34}(A) heterodimers is −7.3 − (−9.3) = +1.8 kcal/mol/dimer. **a**−**a′** pairs that are more stable than A−A have a minus sign, and **a**−**a′** pairs that are less stable than A−A have a plus sign.

Table 3: Difference in the Stability (kcal/mol/dimer) of Reciprocal Heterotypic **a**−**a′** Interactions for the 90 heterotypic **a**−**a′** Interactions Presented in Table 2[a]

protein	A-RR34(A) $\Delta\Delta G_{37}$	A-RR34(I) $\Delta\Delta G_{37}$	A-RR34(V) $\Delta\Delta G_{37}$	A-RR34(L) $\Delta\Delta G_{37}$	A-RR34(N) $\Delta\Delta G_{37}$	A-RR34(T) $\Delta\Delta G_{37}$	A-RR34(S) $\Delta\Delta G_{37}$	A-RR34(K) $\Delta\Delta G_{37}$	A-RR34(R) $\Delta\Delta G_{37}$	A-RR34(E) $\Delta\Delta G_{37}$
B-EE34(A)	A−A	+0.3	−0.1	0	−0.1	+1.2	+1.2	+0.6	+0.6	−0.3
B-EE34(I)	−0.3	I−I	−0.2	+0.1	+0.2	+1.3	+0.4	+0.6	+0.9	−0.7
B-EE34(V)	+0.1	+0.2	V−V	+0.1	+0.2	+1.2	+0.2	+0.7	+0.8	−0.6
B-EE34(L)	0	−0.1	−0.1	L−L	+0.1	+0.9	+0.2	+0.7	+0.8	−0.7
B-EE34(N)	+0.1	−0.2	−0.2	−0.1	N−N	+1.5	+1.6	+0.8	+0.8	−0.4
B-EE34(T)	−1.2	−1.3	−1.2	−0.9	−1.5	T−T	−0.9	−1.3	−0.9	−1.3
B-EE34(S)	−1.2	−0.4	−0.2	−0.2	−1.6	+0.9	S−S	−0.3	−0.4	−1.9
B-EE34(K)	−0.6	−0.6	−0.7	−0.7	−0.8	+1.3	+0.3	K−K	−0.2	−0.5
B-EE34(R)	−0.6	−0.9	−0.8	−0.8	−0.8	+0.9	+0.4	+0.2	R−R	−0.5
B-EE34(E)	+0.3	+0.7	+0.6	+0.7	+0.4	+1.3	+1.9	+0.5	+0.5	E−E

[a] For example, the difference in stability of the B-EE_{34}(T)|A-RR_{34}(I) heterodimer and the (B-EE_{34}(I)|A-RR_{34}(T) heterodimer is [-2.1 − (−0.8)] = −1.3 kcal/mol/dimer. Thus, the difference in the stability of the T−I and I−T **a**−**a′** pairs is −1.3 kcal/mol/dimer and indicates that having T in B-EE_{34}(T) is −1.3 kcal/mol/dimer more stabilizing than having T in A-RR_{34}(T).

Table 4: Coupling Energies ($\Delta\Delta\Delta G$) (kcal/mol/dimer) for the **a**−**a′** Pairs for a Double Mutant Alanine Thermodynamic Cycle

protein	A-RR34(I) $\Delta\Delta\Delta G_{37}$	A-RR34(V) $\Delta\Delta\Delta G_{37}$	A-RR34(L) $\Delta\Delta\Delta G_{37}$	A-RR34(N) $\Delta\Delta\Delta G_{37}$	A-RR34(T) $\Delta\Delta\Delta G_{37}$	A-RR34(S) $\Delta\Delta\Delta G_{37}$	A-RR34(K) $\Delta\Delta\Delta G_{37}$	A-RR34(R) $\Delta\Delta\Delta G_{37}$	A-RR34(E) $\Delta\Delta\Delta G_{37}$
B-EE34(I)	−0.9	+0.4	+0.9	+4.9	+2.2	+2.1	−0.4	+0.4	+1.3
B-EE34(V)	+0.2	−0.7	+0.2	+3.2	+0.3	+1.5	−0.5	−0.2	+0.7
B-EE34(L)	+0.5	+0.2	−0.6	+2.8	+0.6	+1.3	−0.1	+0.1	+0.4
B-EE34(N)	+4.3	+3.0	+2.6	−0.5	+1.3	+0.9	−0.2	−0.1	+1.0
B-EE34(T)	+2.2	+0.8	+1.3	+1.1	+0.2	+0.6	−0.6	−0.2	+0.5
B-EE34(S)	+2.6	+2.6	+2.3	+0.6	+1.1	+0.2	−0.1	+0.1	+0.2
B-EE34(K)	−0.7	−0.5	−0.2	−0.3	−0.3	−0.4	+0.3	+0.8	+0.5
B-EE34(R)	−0.2	−0.3	−0.1	−0.2	+0.1	−0.1	+1.1	+1.2	+0.6
B-EE34(E)	+1.4	+1.1	+0.8	+1.2	+0.3	+0.6	+0.1	+0.2	+2.1
specificity range	−0.9 − +4.3 = 5.2	−0.7 − +3.0 = 3.7	−0.6 − +2.6 = 3.2	−0.5 − +4.9 = 5.4	−0.3 − +2.2 = 2.5	−0.4 − +2.2 = 2.5	−0.6 − +1.1 = 1.7	−0.2 − +1.2 = 1.4	+0.2 − +2.1 = 1.9

a−**a′** pairs with attractive coupling energies include 4 homotypic **a**−**a′** pairs (I, L, V, and N), whereas the remaining 20 pairs are heterotypic **a**−**a′** pairs containing either R or K.

The greatest difference in coupling energies for each amino acid was determined and termed as specificity range. The specificity range for the nine **a**−**a′** pairs was obtained using calculated coupling energies. The amino acids with the greatest difference in coupling energies contribute most to dimerization specificity (Table 4). For example, the most stabilizing coupling energy for isolecuine is −0.9 kcal/mol/dimer for the I−I pair, whereas the least stabilizing coupling energy is +4.3 kcal/mol/dimer for N−I. Coupling energy values for the other 7 heterodimers with A-RR_{34}(I) fall between these two extremes; therefore, the specificity range for the A-RR_{34}(I)| B-RR_{34}(X) heterodimer is −0.9 − +4.3 = 5.2 kcal/mol/dimer. In summary, isoleucine and asparagine have coupling energies with the greatest differences (5.2 and 5.4 kcal/mol/dimer, respectively) and favor homotypic **a**−**a′** pairs. In contrast, the charged amino acids have coupling energies with the least differences (1.4 to 1.9 kcal/mol/dimer) and favor heterotypic **a**−**a′** pairs, suggesting more promiscuous interactions. The difference in coupling energies for reciprocal heterotypic **a**−**a′** pairs is modest, suggesting that these calculations are independent of the overlying **g**↔**e′** salt bridges.

Energetics of Amino Acids in the a Position Interacting with Other Parts of the Coiled-Coil Structure. To evaluate

Table 5: **a**−**a′** Pair Stability (kcal/mol/dimer) Relative to A−A minus α-Helix Propensity, Transfer Free Energy, and **a**−**a′** Coupling Energies[a]

protein	A-RR34(A) $\Delta\Delta G_{37}$	A-RR34(I) $\Delta\Delta G_{37}$	A-RR34(V) $\Delta\Delta G_{37}$	A-RR34(L) $\Delta\Delta G_{37}$	A-RR34(N) $\Delta\Delta G_{37}$	A-RR34(T) $\Delta\Delta G_{37}$	A-RR34(S) $\Delta\Delta G_{37}$	A-RR34(K) $\Delta\Delta G_{37}$	A-RR34(R) $\Delta\Delta G_{37}$	A-RR34(E) $\Delta\Delta G_{37}$
B-EE34(A)	0	−2.4	−1.7	−0.4	−3.0	+0.1	+0.5	−0.3	+0.6	−0.1
B-EE34(I)	−2.7	−5.1	−4.4	−3.1	−5.7	−2.6	−2.2	−3.0	−2.1	−2.8
B-EE34(V)	−1.6	−4.0	−3.3	−2.0	−4.6	−1.5	−1.1	−1.9	−1.0	−1.7
B-EE34(L)	−0.4	−2.8	−2.1	−0.8	−3.4	−0.3	+0.1	−0.7	+0.2	−0.5
B-EE34(N)	−2.9	−5.3	−4.6	−3.3	−5.9	−2.8	−2.4	−3.2	−2.3	−3.0
B-EE34(T)	−0.9	−3.3	−2.8	−1.3	−3.9	−0.8	−0.4	−1.2	−0.5	−1.0
B-EE34(S)	−0.7	−3.1	−2.4	−1.1	−3.7	−0.6	−0.2	−1.0	−0.1	−0.8
B-EE34(K)	−0.9	−3.3	−2.6	−1.3	−3.9	−0.8	−0.4	−1.2	−0.3	−1.0
B-EE34(R)	−0.6	−3.0	−2.3	−1.0	−3.6	−0.5	−0.1	−0.9	0.0	−0.7
B-EE34(E)	+0.2	−2.2	−1.5	−0.2	−2.8	+0.3	+0.7	−0.1	+0.8	+0.1

[a] α-helix propensities (*34*), transfer free energies (*29*), and the **a**−**a′** pair coupling energy were subtracted from the stability of an **a**−**a′** pair relative to A−A to identify additional energies in the **a**−**a′** pair.

Table 6: Coupling Energy (kcal/mol/dimer) Difference between Two Monomers with Different Amino Acids in the **a** Position Forming Either Two Homotypic or Two Heterotypic **a**−**a′** Pairs[a]

amino acid	I	V	L	N	T	S	K	R	E
I	**								
V	+1.1	**							
L	+1.5	+0.9	**						
N	+10.6	+3.7	+3.3	**					
T	+2.6	+0.8	+1.2	+1.35	**				
S	+2.7	+2.3	+2.0	+0.9	+0.65	**			
K	−0.3	0	0	−0.15	−0.7	−0.5	**		
R	0	−0.5	−0.3	−0.2	−0.75	−0.6	+0.2	**	
E	+1.3	+0.2	−0.15	+0.3	−0.75	−0.75	−0.9	−1.25	**

[a] A positive number indicates that two homotypic **a**−**a′** pairs are preferred. For example, two monomers, one containing N and the other containing I in the **a** position could form either N−N and I−I **a**−**a′** pairs or N−I and I−N **a**−**a′** pairs. The difference in the coupling energy between these two possibilities is (N−N + I−I) − (N−I + I−N) or (−0.5 + −0.9) − (+4.3 + +4.9) = +10.6/two dimers or +5.3 kcal/mol/dimer. Thus, these two amino acids prefer to form homotypic N and I **a**−**a′** pairs.

potential energetic interactions between an amino acid in the **a** position and other amino acid in the coiled-coil structure, three energy terms, α-helix propensities (*34*), transfer free energies (*29*), and the **a**−**a′** pair coupling energy (Table 5), were subtracted from the stability of an **a**−**a′** pair relative to that of A−A. Any remaining energies may represent interactions of amino acids in the **a** position with other parts of the coiled-coil structure. When examining **a**−**a′** pairs containing one alanine, only three amino acids contribute more than 1 kcal/mol to additional stability that is not accounted for by these three energy terms. They are asparagines and the two *β*-branched aliphatic amino acids isoleucine and valine. This indicates that the other six amino acids are not energetically interacting with additional components of the coiled-coil structure.

Do Amino Acids Prefer to Form Homotypic or Heterotypic **a**−**a′** *Pairs? Difference in Coupling Energies.* To evaluate whether two leucine zipper monomers containing different amino acids in the **a** position would preferentially form homodimers or heterodimers, the difference in the coupling energy between these two possibilities was determined (Table 6). The most extreme example of two amino acids regulating dimer preference has to do with I and N. They strongly prefer to form homotypic **a**−**a′** pairs (*1*). The coupling energies for the two homotypic **a**−**a′** interactions (I−I and N−N) are −0.9 and −0.5 kcal/mol, respectively. The coupling energies for the two heterotypic **a**−**a′** pairs (I−N and N−I) are +4.3 and +4.9 kcal/mol, respectively. Thus, the energetic difference between the two homodimers and the two heterodimers is 10.6 kcal/mol/two dimers or 5.3 kcal/mol/dimer, indicating that N and I prefer to form N−N and I−I homotypic **a**−**a′** pairs.

Of the 36 reciprocal heterotypic **a**−**a′** pairs with measured coupling energies, 19 prefer to form homodimers, 14 prefer to form heterodimers, and 3 **a**−**a′** pairs have no preference. Several general conclusions are clear. The aliphatic (I, V, and L) and polar (N, S, and T) amino acids prefer to form homotypic **a**−**a′** pairs instead of heterotypic **a**−**a′** pairs with any of the other aliphatic or polar amino acids. In contrast, the three charged amino acids (E, K, and R) generally prefer to form heterotypic pairs. The strongest stabilizing heterodimer coupling energy for the three charged amino acids (K, R, and E) is with the polar amino acids serine and theronine by ∼0.7 kcal/mol/dimer. Both the basic and acidic amino acids interact similarly with serine and threonine.

DISCUSSION

We present the thermal stability of 100 heterodimers that contain all possible **a**−**a′** pairs for 10 amino acids (I, V, L, N, A, K S, T, E, and R) commonly observed in the B-ZIP leucine zipper **a** position. This includes the stability of 36 heterodimers for 6 amino acids (I, V, L, N, A, and K) previously described (*1*) and 64 new heterodimers including the 4 amino acids (S, T, E, and R). A double mutant alanine thermodynamic cycle was used to determine **a**−**a′** pair coupling energies to evaluate which **a**−**a′** pairs encourage specific dimerization partners. Isoleucine and asparagine show the greatest difference in coupling energies, indicating that they contribute the most to dimerization specificity and prefer to homodimerize. The three charged amino acids (K, R and E) show the least difference in coupling energies (1.4 to 1.9 kcal/mol/dimer), suggesting that they contribute the least to dimerization specificity (Table 3) and prefer to heterodimerize. Most of the measured **a**−**a′** pairs had repulsive (positive) coupling energies. We were able to determine their stability only by embedding the repulsive **a**−**a′** pairs in a larger coiled-coil structure with stabilizing heptads on both the *N*- and *C*-termini.

Each of the 10 amino acids was placed in the **a** position in both the B-EE$_{34}$(X) and the A-RR$_{34}$(X) protein background to produce 20 proteins and were mixed to produce 100 heterodimers. The 90 heterotypic **a**−**a′** pairs contain recipro-

cal versions for each of 45 heterotypic **a**−**a′** pairs that structurally differ in the orientation of the overlying electrostatically attractive **E↔R g↔e′** pair. The reciprocal heterotypic **a**−**a′** pairs containing aliphatic amino acids (I, V, and L) and the polar N are energetically similar (e.g., the I−N and N−I interactions differ by only 0.2 kcal/mol/dimer), suggesting that these amino acids are not interacting with the overlaying attractive **E↔R** pair. Reciprocal **a**−**a′** interactions containing T and S, however, show the greatest difference; in the nine heterotypic **a**−**a′** pairs containing T, the **a**−**a′** pairs are 0.9 to 1.5 kcal/mol/dimer more stable when T is in B-EE_{34}(T) than when it is in A-RR_{34}(T). Similarly, when S is in B-EE_{34}(S), the **a**−**a′** pairs are 0.2 to 1.9 kcal/mol/dimer more stable than when S is in A-RR_{34}-(S).

The coupling energies were used to calculate a preference for two monomers containing different amino acids in the **a** position to either form a homodimer or a heterodimer. A similar approach was performed computationally and the results verified experimentally (*35*). Havranek and Harbury identified groups of amino acids in the hydrophobic core defined as the **g**, **a**, **d**, and **e** positions that were able to drive heterodimeriztion. For example, a tryptophane in the **g** position interacts interhelically with the cavity created by a glycine in the **a** position.

To evaluate potential energetic interactions between an amino acid in the **a** position and other amino acids in the coiled-coil structure, we subtracted α-helix propensities (*34*), transfer free energies (*29*), and the **a**−**a′** pair coupling energy (Table 6) from the stability of an **a**−**a′** pair relative to that of A−A. A potential opportunity for an amino acid in the **a** position is to interact intrahelically with the leucines in the **d** positions. The *β*-branched amino acids, valine and isoleucine, show approximately −1.5 and −2.5 kcal/mol/dimer additional energy, which is larger than that observed for the non-*β*-branched leucine with −0.4 kcal/mol/dimer. These results are qualitatively consistent with work that has examined intrahelical interactions between aliphatic amino acids (*36*, *37*). The energetic significance of intrahelical hydrophobic interactions is clearly shown in recent work suggesting that three consecutive hydrophobic amino acids are required in the hydrophobic core of a coiled coil to produce stabilizing interactions (*38*).

An enigma is the 3 kcal/mol/dimer of residual energy for asparagine that is observed after these three energy terms are subtracted. Part of this could be that including a 1.3 kcal/mol transfer free energy for buried asparagine may be incorrect because asparagine is not really buried. In the N−A pair, a water molecule could be occupying the cavity caused by the small alanine side chain. This could explain the small calculated coupling energy for N−N of 0.9 kcal/mol/dimer because asparagines in the N−A pair could be forming a hydrogen bound with the water. Additionally, the asparagines could be forming hydrogen bonds with the overlying charged amino acids that create attractive interhelical electrostatic **g↔e′** interactions as is observed in the crystal structure of a chimeric cortexillinI/GCN4 coiled-coil peptide (*39*).

Recently, Keating's group generated physical models of B-ZIP leucine zippers that were able to mimic the dimerization properties of a global analysis of human B-ZIP proteins (*25*). These models recapitulated the coupling energies experimentally identified for the surface **g↔e′** interactions but were not able to recapitulate the **a**−**a′** coupling energies we have previously reported. They calculated coupling energies of approximately zero for **a**−**a′** pairs containing asparagine and an aliphatic amino acid, whereas we measured destabilizing coupling energies of 3 to 4 kcal/mol/dimer. This may reflect subtle details about the backbone geometry, where small differences have large effects on amino acid packing or calculations underestimating the burial of asparagine in the hydrophobic core.

The coupling energies described here apply only to the particular heptad examined. We have previously shown that the stabilizing contribution of leucine in the **d** position is dependent on the structural details of the particular heptad. In a canonical heptad with valine in the two flanking **a** positions, leucine contributes 4.6 kcal/mol/monomer more to stability than alanine. However, when leucine in the **d** position is two heptads further *N*-terminal and is surrounded by alanine in the *N*-terminal **a** position and asparagine in the *C*-terminal **a** position, it only contributes 2.1 kcal/mol/monomer more than alanine (*17*). Two open issues include what the rules are for **a**−**a′** interactions without overlying attractive **g↔e′** pairs and in coiled-coil structures that are not optimized for stability.

A global analysis of human B-ZIP dimerization (*40*) indicated that the quantitative rules that we have previously generated for leucine zipper dimerization specificity using **g↔e′** and **a↔a′** coupling energies give a reasonably good prediction of their experimental results of human B-ZIP dimerization specificity. Computational analyses that include correlations beyond **g↔e′** and **a↔a′** coupling energies are more predictive, indicating that additional interhelical interactions regulate dimerization specificity (*24*). We hope these data will make computer predictions even more valuable.

The data presented here should be useful for coiled-coil design (*23*, *41*), predicting coiled-coil dimerization specificity (*24*) and calibrating computation models of coiled-coil stability (*25*).

ACKNOWLEDGMENT

We thank Chris Deppmann for help with Figure 2. We thank Amy Keating for thoughtful insights.

SUPPORTING INFORMATION AVAILABLE

Spectra from 260 to 200 nm and thermal denaturation profiles for all 100 heterodimers. This material is available free of charge via the Internet at http://pubs.acs.org.

REFERENCES

1. Acharya, A., Ruvinov, S. B., Gal, J., Moll, J. R., and Vinson, C. (2002) A heterodimerizing leucine zipper coiled coil system for examining the specificity of a position interactions: amino acids I, V, L, N, A, and K, *Biochemistry 41*, 14122−14131.
2. Crick, F. (1953) The packing of α- helicies: simple coiled-coils, *Acta Crystallogr. 6*, 689−697.
3. O'Shea, E. K., Klemm, J. D., Kim, P. S., and Alber, T. (1991) X-ray structure of the GCN4 leucine zipper, a two-stranded, parallel coiled-coil, *Science 254*, 539−544.
4. Hodges, R. S. (1996) Boehringer Mannheim award lecture 1995. La conference Boehringer Mannheim 1995. De novo design of alpha-helical proteins: basic research to medical applications, *Biochem. Cell Biol. 74*, 133−154.
5. Lupas, A. (1996) Coiled coils: new structures and new functions, *Trends Biochem Sci. 21*, 375−382.

6. McLachlan, A., and Stewart, M. (1975) Tropomyosin coiled-coil interactions: evidence for an unstaggered structure, *J. Mol. Biol. 98*, 293−304.
7. Thompson, K. S., Vinson, C. R., and Freire, E. (1993) Thermodynamic characterization of the structural stability of the coiled-coil region of the bZIP transcription factor GCN4, *Biochemistry 32*, 5491−5496.
8. Vinson, C., Myakishev, M., Acharya, A., Mir, A. A., Moll, J. R., and Bonovich, M. (2002) Classification of human B-ZIP proteins based on dimerization properties, *Mol. Cell Biol. 22*, 6321−6335.
9. Landschultz, W. H., Johnson, P. F., and McKnight, S. L. (1988) The leucine zipper: a hypothetical structure common to a new class of DNA binding proteins, *Science 240*, 1759−1764.
10. Glover, J. N., and Harrison, S. C. (1995) Crystal structure of the heterodimeric bZIP transcription factor c-Fos-c-Jun bound to DNA, *Nature 373*, 257−261.
11. Steinmetz, M. O., Stock, A., Schulthess, T., Landwehr, R., Lustig, A., Faix, J., Gerisch, G., Aebi, U., and Kammerer, R. A. (1998) A distinct 14 residue site triggers coiled-coil formation in cortexillin I, *EMBO J. 17*, 1883−1891.
12. Lee, D. L., Lavigne, P., and Hodges, R. S. (2001) Are trigger sequences essential in the folding of two-stranded alpha-helical coiled-coils? *J. Mol. Biol. 306*, 539−553.
13. Zhou, N. E., Kay, C. M., and Hodges, R. S. (1994) The net energetic contribution of interhelical electrostatic attractions to coiled-coil stability, *Protein Eng. 7*, 1365−1372.
14. Wagschal, K., Tripet, B., Lavigne, P., Mant, C., and Hodges, R. S. (1999) The role of position a in determining the stability and oligomerization state of alpha-helical coiled coils: 20 amino acid stability coefficients in the hydrophobic core of proteins, *Protein Sci. 8*, 2312−2329.
15. Tripet, B., Wagschal, K., Lavigne, P., Mant, C. T., and Hodges, R. S. (2000) Effects of side-chain characteristics on stability and oligomerization state of a de novo-designed model coiled-coil: 20 amino acid substitutions in position "d", *J. Mol. Biol. 300*, 377−402.
16. Krylov, D., Mikhailenko, I., and Vinson, C. (1994) A thermodynamic scale for leucine zipper stability and dimerization specificity: e and g interhelical interactions, *EMBO J. 13*, 1849−1861.
17. Moitra, J., Szilak, L., Krylov, D., and Vinson, C. (1997) Leucine is the most stabilizing aliphatic amino acid in the d position of a dimeric leucine zipper coiled coil, *Biochemistry 36*, 12567−12573.
18. Krylov, D., Barchi, J., and Vinson, C. (1998) Inter-helical interactions in the leucine zipper coiled coil dimer: pH and salt dependence of coupling energy between charged amino acids, *J. Mol. Biol. 279*, 959−972.
19. Deppmann, C. D., Acharya, A., Rishi, V., Wobbes, B., Smeekens, S., Taparowsky, E. J., and Vinson, C. (2004) Dimerization specificity of all 67 B-ZIP motifs in *Arabidopsis thaliana*: a comparison to Homo sapiens B-ZIP motifs, *Nucleic Acids Res. 32*, 3435−3445.
20. Harbury, P. B., Zhang, T., Kim, P. S., and Alber, T. (1993) A switch between two-, three-, and four-stranded coiled coils in GCN4 leucine zipper mutants, *Science 262*, 1401−1407.
21. Potekhin, S. A., Medvedkin, V. N., Kashparov, I. A., and Venyaminov, S. (1994) Synthesis and properties of the peptide corresponding to the mutant form of the leucine zipper of the transcriptional activator GCN4 from yeast, *Protein Eng. 7*, 1097−1101.
22. Gonzalez, L., Jr., Woolfson, D. N., and Alber, T. (1996) Buried polar residues and structural specificity in the GCN4 leucine zipper, *Nat. Struct. Biol. 3*, 1011−1018.
23. Krylov, D., Olive, M., and Vinson, C. (1995) Extending dimerization interfaces: the bZIP basic region can form a coiled coil, *EMBO J. 14*, 5329−5337.
24. Fong, J. H., Keating, A. E., and Singh, M. (2004) Predicting specificity in bZIP coiled-coil protein interactions, *Genome Biol. 5*, R11.
25. Grigoryan, G., and Keating, A. E. (2006) Structure-based prediction of bZIP partnering specificity, *J. Mol. Biol. 355*, 1125−1142.
26. Moll, J. R., Olive, M., and Vinson, C. (2000) Attractive interhelical electrostatic interactions in the proline- and acidic-rich region (PAR) leucine zipper subfamily preclude heterodimerization with other basic leucine zipper subfamilies, *J. Biol. Chem. 275*, 34826−34832.
27. Studier, F. W., and Moffatt, B. A. (1986) Use of bacteriophage T7 RNA polymerase to direct selective high-level expression of cloned genes, *J. Mol. Biol. 189*, 113−130.
28. Olive, M., Krylov, D., Echlin, D. R., Gardner, K., Taparowsky, E., and Vinson, C. (1997) A dominant negative to activation protein-1 (AP1) that abolishes DNA binding and inhibits oncogenesis, *J. Biol. Chem. 272*, 18586−18594.
29. Fauchere, J. L., Charton, M., Kier, L. B., Verloop, A., and Pliska, V. (1988) Amino acid side chain parameters for correlation studies in biology and pharmacology, *Int. J. Pept. Protein Res. 32*, 269−278.
30. Chen, Y. H., Yang, J. T., and Chau, K. H. (1974) Determination of the helix and beta form of proteins in aqueous solution by circular dichroism, *Biochemistry 13*, 3350−3359.
31. Lau, S. Y., Taneja, A. K., and Hodges, R. S. (1984) Synthesis of a model protein of defined secondary and quaternary structure. Effect of chain length on the stabilization and formation of two-stranded alpha-helical coiled-coils, *J. Biol. Chem. 259*, 13253−13261.
32. Cooper, T. M., and Woody, R. W. (1990) The effect of conformation on the CD of interacting helices: a theoretical study of tropomyosin, *Biopolymers 30*, 657−676.
33. Serrano, L., Horovitz, A., Avron, B., Bycroft, M., and Fersht, A. R. (1990) Estimating the contribution of engineered surface electrostatic interactions to protein stability by using double-mutant cycles, *Biochemistry 29*, 9343−9352.
34. O'Neil, K. T., and DeGrado, W. F. (1990) A thermodynamic scale for the helix-forming tendencies of the commonly occurring amino acids, *Science 250*, 646−651.
35. Havranek, J. J., and Harbury, P. B. (2003) Automated design of specificity in molecular recognition. *Nat. Struct. Biol. 10*, 45−52.
36. Creamer, T. P., and Rose, G. D. (1994) Alpha-helix-forming propensities in peptides and proteins, *Proteins 19*, 85−97.
37. Padmanabhan, S., and Baldwin, R. L. (1994) Tests for helix-stabilizing interactions between various nonpolar side chains in alanine-based peptides, *Protein Sci. 3*, 1992−1997.
38. Lu, S. M., and Hodges, R. S. (2004) Defining the minimum size of a hydrophobic cluster in two-stranded alpha-helical coiled-coils: effects on protein stability, *Protein Sci. 13*, 714−726.
39. Lee, D. L., Ivaninskii, S., Burkhard, P., and Hodges, R. S. (2003) Unique stabilizing interactions identified in the two-stranded alpha-helical coiled-coil: crystal structure of a cortexillin I/GCN4 hybrid coiled-coil peptide, *Protein Sci. 12*, 1395−1405.
40. Newman, J. R., and Keating, A. E. (2003) Comprehensive identification of human bZIP interactions with coiled-coil arrays, *Science 300*, 2097−2101.
41. Lupas, A. N., and Gruber, M. (2005) The structure of alpha-helical coiled coils, *Adv. Protein Chem. 70*, 37−78.

BI060822U